Small-molecule MDM2-p53 inhibitors - recent advances

Bian Zhang, Bernard T. Golding, Ian R. Hardcastle

Newcastle Cancer Centre, School of Chemistry, Bedson Building, Newcastle University, NE1 7RU

Defined Keywords

p53	the tumour suppressor protein p53, a signalling node in the cellular stress and DNA damage response
MDM2	Mouse double minute 2 protein, an E3 ligase and negative regulator of p53
Nutlins	A series of imidazoline based MDM2-p53 inhibitors, including RG7112
Spirooxindoles	A series of MDM2-p53 inhibitors, including SAR405838
Cyanopyrrolidines	A series of MDM2-p53 inhibitors, including RG7388
Piperidinones	A series of MDM2-p53 inhibitors, including AMG232

Abstract

Potent and selective small-molecule inhibitors of the p53-MDM2 interaction intended for the treatment of p53 wild type tumours have designed and optimised in a number of chemical series. This review details recent disclosures of compounds in advanced optimisation and features key series that have given rise to clinical trial candidates. The structure-activity relationships for inhibitor classes are discussed with reference to X-ray structures, and common structural features are identified.

Introduction

The *TP53* gene encodes a 53 KDa protein – the tumour suppressor p53,[1] which acts as a node in cell signalling, becoming activated following posttranslational modifications such as phosphorylation and acetylation.[2] Activated p53 transcribes a number of genes, the cognate proteins of which are involved in DNA repair, senescence and apoptosis.[3] The oncoprotein MDM2, first found to be associated with p53 protein in human sarcomas, is another product of p53 transcription.[4,5] MDM2 inhibits the activity of p53 directly, by binding to the p53 transactivation domain and by acting as an E3-ubiquitin ligase, tagging the complex for proteasomal degradation.[6,7] MDM2 is a transcribed by activated p53, so the two proteins are linked in an autoregulatory feedback loop (Figure 1). Gene amplification of *MDM2* giving rise to overexpression

of MDM2 protein has been observed in tumour samples taken from common sporadic cancers. Overall, around 50% of tumours are p53 wild type and 10% of tumours have *MDM2* amplification, with the highest incidence found in hepatocellular carcinoma (44%), lung (15%), sarcomas and osteosarcomas (28%), and Hodgkin disease (67%).[8]

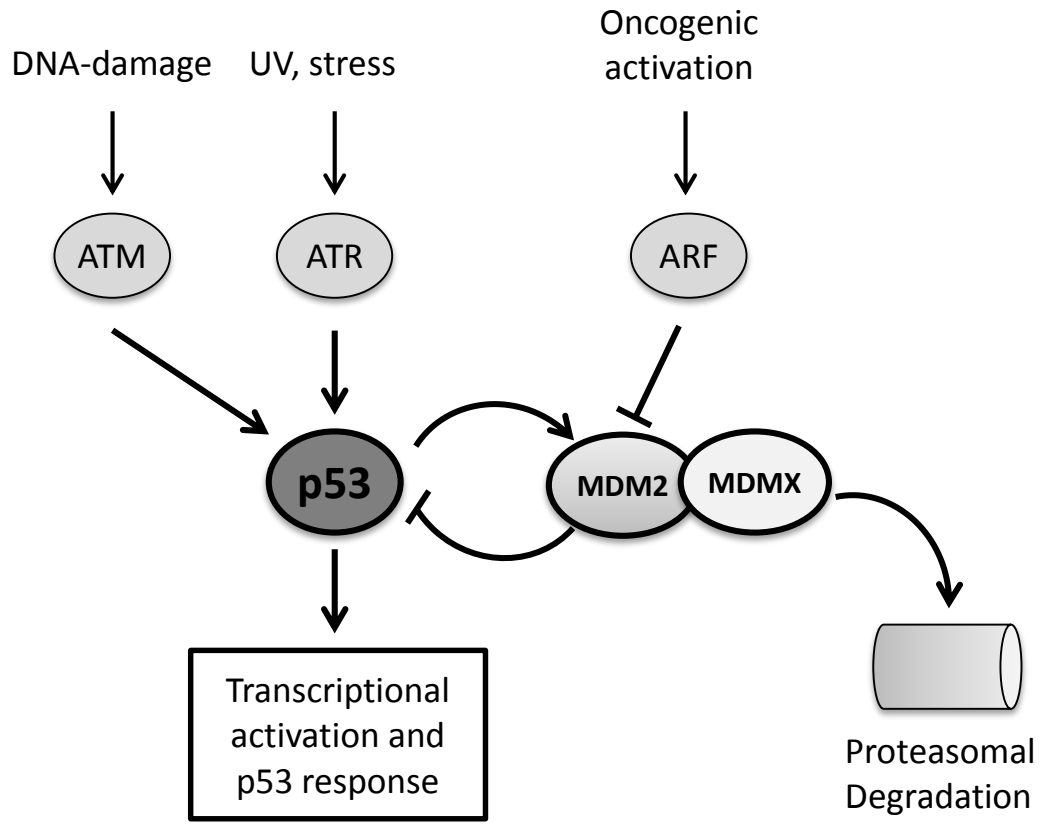

Figure 1: Cell signalling pathways regulating p53 and MDM2.

The tractability of the MDM2-p53 protein-protein interaction (PPI) to inhibition by small molecules was first demonstrated by experiments with peptide libraries.[9,10] A peptide that structurally corresponded to the p53 transactivation domain showed modest inhibitory activity. This strategy resulted in the identification of the potent 8-mer AP peptide (IC_{50} = 5 nM).[11] The X-ray structure of an 11-mer peptide bound to MDM2 (pdb: 1YCR, Figure 8) showed that this p53-like α-helical peptide binds to MDM2 in a deep groove lined with hydrophobic residues.[12] Three lipophilic p53 residues (Phe19, Trp23, and Leu26) bind deep within the groove. Two hydrogen bonds are formed between the Gln72 side chain of MDM2 and the backbone amide of Phe19 and between the backbone carbonyl of Leu54 from MDM2 and the p53 Trp23 indole NH. Overall, the relative small size and cavity-like shape of the binding site on MDM2 are characteristics favourable for insertion of small-molecule inhibitors.

The therapeutic hypothesis for disruption of the MDM2-p53 interaction with small-molecules is that potent inhibition will result in the release of p53 from MDM2 inactivation. In tumours, free p53 is proposed to sense pre-existing DNA-damage or oncogenic signalling resulting in apoptosis. In normal cells, p53 activation can result in activation of non-apoptotic pathways such as DNA-repair and senesence.

A number of previous reviews have described the development of inhibitor chemotypes, including isoindolinones discovered in our laboratory.[13-16] This review will focus on recently disclosed inhibitors and, in particular, the development of the series that have recently entered clinical trials. These first generation MDM2-p53 clinical trial candidates each demonstrate excellent potency and their X-ray co-crystal structures allow a detailed appraisal of structure-activity relationships. To date, whilst only one clinical trial has been published in full (RG7112) [17], the results of other trials are eagerly awaited.

Nutlin analogues

The *cis*-imidazoline class of inhibitors dubbed 'Nutlins', gave the first reported X-ray structure of MDM2 bound to a small-molecule ligand (Nutlin-2, **1a**) and the first *in vivo* anti-tumour activity (Nutlin-3a, **1b**).[18] The potency and selectivity of **1b** has made it the tool compound of choice for many studies investigating the role of MDM2 and p53 in cells. Further development of the series sought to improve the pharmacological profile of the inhibitors, whilst retaining potency and cellular selectivity for p53 wild-type over mutant cell-lines.[19] In particular, metabolic liabilities at the imidazoline heterocycle and the 4-methoxy group were addressed by the introduction of two *cis*-methyl groups, and replacement with a *tert*-butyl group, respectively, giving **2a**, that retained similar potency to **1b** (Table 1). Additional potency was gained by modifying the hydrophilic side-chain and the pharmacokinetic (PK) profile was modulated (**2b-f**). The X-ray co-crystal structure of MDM2 with **2c** (pdb 4IPF, Figure 8) showed the same binding mode as with **1a** with the methylsulfone side chain making no additional interactions with the protein. Compound **2c** (RG7112) was chosen as having the optimal profile for progression to clinical trials .[20]

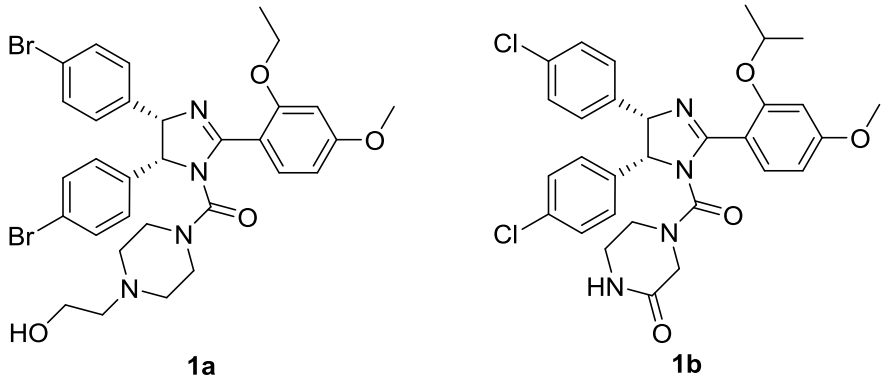

Figure 2: Chemical structures of Nutlin-2 (**1a**) and Nutlin-3a (**1b**).

Table 1: MDM2-p53 inhibitory activity and PK parameters for Nutlin analogues **1a**, **1b** and **2a-f**.

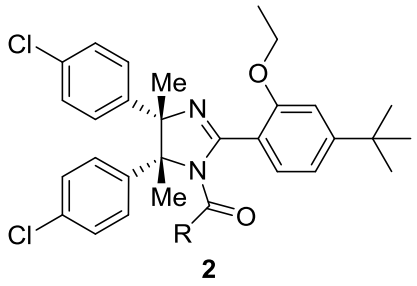

Compound	R_3	IC_{50}[a] (μM)	AUC_{last} (μg·h/mL)[b]	$t_{1/2}$ (h)[b]	Ref
1a	-	0.14[c]	N/A	N/A	[18]
1b	-	0.09	N/A	N/A	[18]
2a	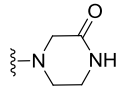	0.052	N/A	N/A	[19]
2b	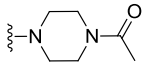	0.023	64.9	2.4	[19]
2c	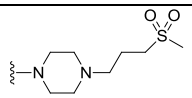	0.018	251.2	8.8	[19]
2d	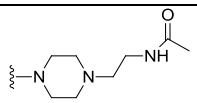	0.033	136.5	2.3	[19]
2e	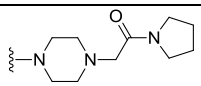	0.014	8.3	4.7	[19]
2f	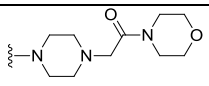	0.018	N/A	N/A	[19]

a) Homogeneous time-resolved fluorescence (HTRF) assay; b) Mouse PK, single dose 50 mg/kg ; c) Measured as racemate

A series dihydroimidazothiazole derivatives **3** was developed using knowledge from the Nutlins. The introduction of the bicyclic unit allows the 3-isopropyl group to be fixed in the optimum position for access to the Phe19 pocket, which is occupied by the ethoxy group of **2c**.[21] The addition of a 6-methyl group to the ring gave **3b**, with similar potency to Nutlin **1b**. Further elaboration of the 4 position amide gave additional potency, e.g. **3d** (Table 2).[22] Analysis of the X-ray structure of **3d** bound to MDM2 showed that the amide side-chain binds into a groove on the surface of the protein that is formed by the movement of a flexible loop region. The authors posit that the pyrrolidine-2-carboxamide substituent offers the ability to modulate the pharmacological properties of the compounds, e.g. **3e**.

Table 2: MDM2-p53 inhibitory activity for dihydroimidazothiazoles **3**.[21]

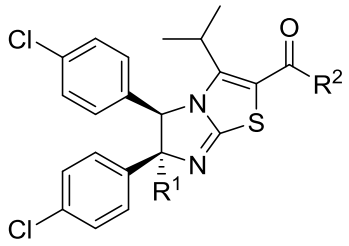

Compound	R^1	R^2	IC_{50} (μM)[a]
3a	H	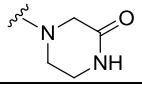	0.16
3b	Me	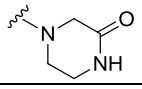	0.092
3c	Me		0.026
3d	Me	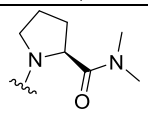	0.0092
3e	Me	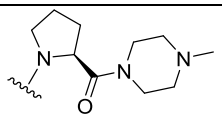	0.023

a) ELISA assay

Spirooxindole Series

The spirooxindole series, e.g. MI-63 (**4a**), was discovered by computational substructure searching for tryptophan mimetics.[23] Elaboration of the amide group and addition of a 5-fluoro group led to

4b, which has low nanomolar affinity for MDM2 and showed *in vivo* anti-tumour activity.[24] Importantly, **4b** was found to epimerise in solution in the presence of cerium (IV) ammonium nitrate to a mixture of stereoisomers including **5a**, which displayed improved affinity for MDM2.[25] With this in mind, an additional series of amide derivatives with the more stable stereochemistry was prepared using 3-aminocycloalkanols (Table 3).[26] A number of compounds (**5b-g**) were identified with good cell free and cellular potency. In particular, SAR405838 (**5b**) displayed excellent MDM2 binding affinity and growth inhibitory activity. The X-ray co-crystal structure of **5b** bound to MDM2 showed the amide side-chain carbonyl group makes a hydrogen bond to His96, and refolding of the MDM2 N-terminus was observed. The PK properties of **5b-g** profiled *in vitro* using mouse, rat and human liver microsomes, consequently **5b** was selected for *in vivo* evaluation. Pharmacodynamics (PD) were studied by Western blotting of tumour extracts, probing for p53 and apoptotic markers, i.e. cleaved PARP and caspase. Importantly, a 100 mg/kg single oral dose of **5b** induced complete tumour regression in SJSA-1 mouse xenografts, resulting in the selection of SAR405838 (**5b**) as the clinical candidate from the spirooxindole series.

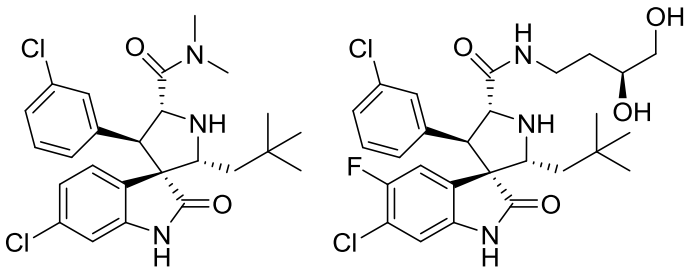

Figure 3: Chemical structures of MI-63 (**4a**) and MI-219 (**4b**)

Table 3: MDM2-p53 inhibitory activity and growth inhibitory activity of spirooxindoles **4b** and **5**

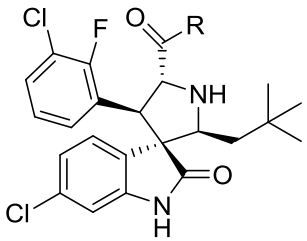

5

Compound	R	MDM2 K_i (nM)[a]	SJSA-1 cell line IC_{50} (μM)
4b	-	10.5 ± 2.0	0.95 ± 0.16[b]
5a	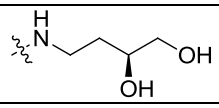	0.86 ± 0.11	0.63 ± 0.04[b]
5b (SAR405838)	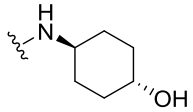	0.88 ± 0.18	0.09 ± 0.02
5c	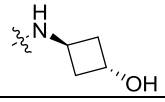	0.61 ± 0.10	0.24 ± 0.05
5d	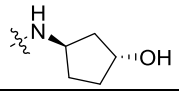	0.62 ± 0.05	0.20 ± 0.02
5e	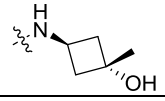	0.97 ± 0.3	0.60 ± 0.16
5f	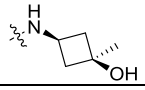	0.44 ± 0.22	0.08 ± 0.02
5g	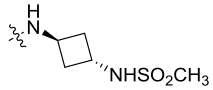	0.62 ± 0.19	0.25 ± 0.04

a) Fluorescence polarisation assay; b) 48 h incubation

RG7388 series

The Roche group sought to address the stereochemical and conformational complexities encountered with the spirooxindole series by replacement of the spirocyclic amide with the simpler and more flexible cyanopyrrolidine core (**6**, Table 4).[27] The cyanopyrrolidine **6a** bearing similar substituents to MI-219 (**4b**), showed good MDM2 binding affinity and modest cellular activity. Introduction of a fluoro substituent at the 2-position of each phenyl ring was found to improve binding to MDM2 (**6b**), but both compounds showed poor oral bioavailability and rapid clearance in mice. Modifications to the amide side chain were introduced to improve the PK profile and remove a possible metabolic hot-spot. Interestingly, these modifications also had a significant effect on the cellular potency of the compounds, and a 4-benzenecarboxylic moiety gave improved PK and cellular

potency, e.g. **6c**. Further optimisation focussed on the introduction of groups with distinct electronic properties, i.e. methoxy and fluoro, at the 2- and 3-positions (**6d-g**). The introduction of an *ortho*-methoxy group, **6g** (RG7388), gave improved MDM2 binding affinity, cellular potency and selectivity. Compound **6g** showed *in vivo* activity in an SJSA-1 xenograft model, and achieved complete tumour regression at the 25 mg/kg dose, with a favourable PK profile. RG7388 (**6g**) was selected as a second generation MDM2-p53 clinical trial candidate owing to its improved potency, cellular selectivity and PK properties over RG7112 (**2g**) .

Table 4: MDM2-p53 inhibitory activity and growth inhibitory activity of cyanopyrroles **6**

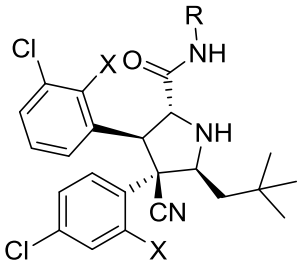

6

Compound	X	R	IC_{50}[a] (nM)	GI_{50} (μM)[b]	CL (mL/min/kg)	$T_{1/2}$ (h)	*F* (%)[c]
6a	H	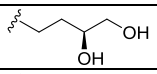	196	2.8	52.9	0.44	6.2
6b	F	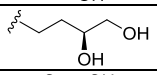	74	2.1	51.7	0.52	3.6
6c	F	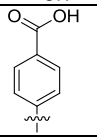	22	0.11	13.8	4.34	83
6d	F	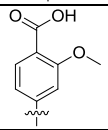	20	0.07	21.8	4.8	56
6e	F	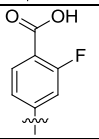	21	0.21	18.4	4.4	49
6f	F	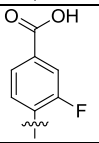	25	0.27	11.5	3.1	100
6g (RG7388)	F	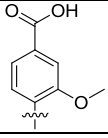	6	0.03	10.3	1.6	80

a) HTRF assay; b) Average GI_{50} for SJSA-1, RKO, and HCT-116 lines (p53wt); c) oral bioavailability

In an alternative approach, starting from the oxindole (**7**), a *de-novo* design hit, structure-based design suggested a spirooxindole scaffold similar to **5**.[28] Structural features taken from **6b** were

incorporated into the new scaffold giving RG8994 (**8**), which exhibited excellent MDM2 binding affinity, cellular activity, and PK profile, comparable with **6b**. Compound **8** showed impressive *in vivo* activity in an SJSA-1 xenograft model, inducing tumour regression with 6.25 mg/kg daily dosing.

Further investigations from RG8994 (**8**) focussed on bioisosteric replacement of the oxindole ring with 5- and 6-membered heterocycles.[29] Key examples RO2468 (**9**) and RO5353 (**10**) showed excellent MDM2 binding affinity (IC_{50} = 6 and 7 nM, respectively) and impressive cellular activity and selectivity (GI_{50} = 15 and 7 nM, respectively). Both compounds presented excellent mouse PK properties, and showed tumour regression in SJSA-1 xenografts at 10 mg/kg daily dosing.

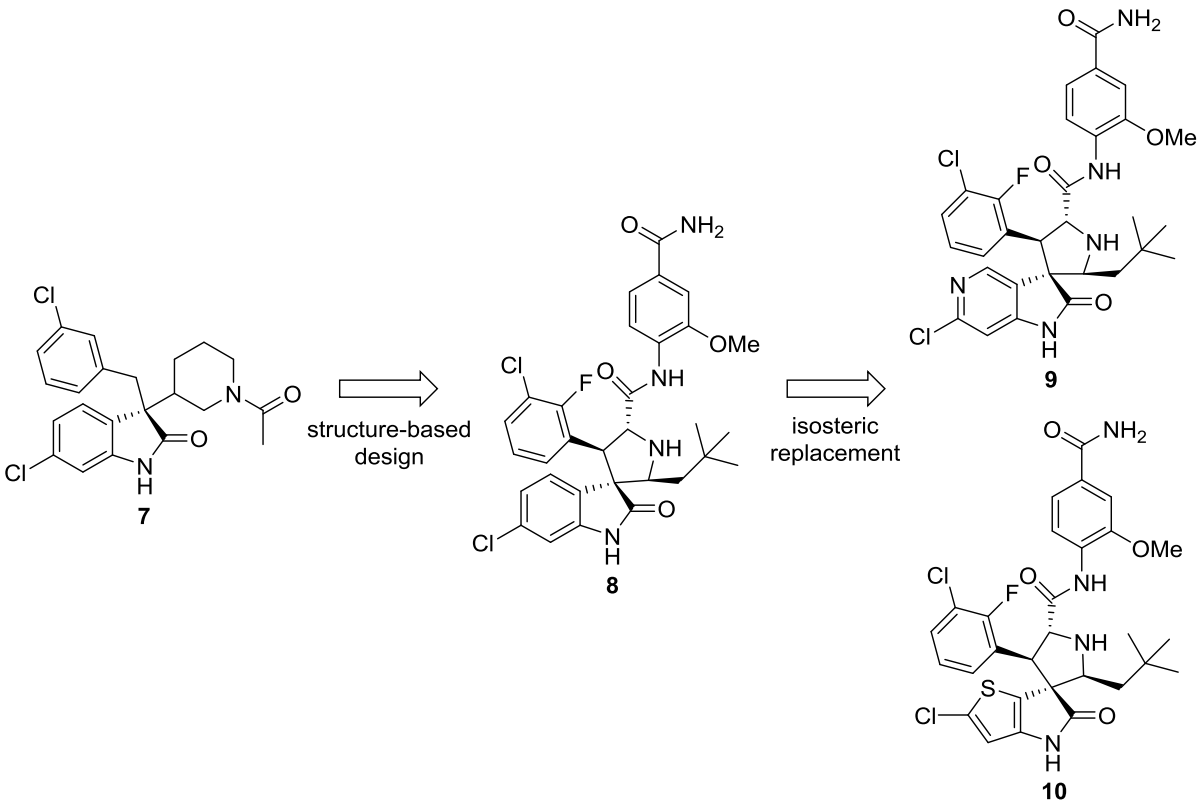

Figure 4: Schematic for the design evolution of spirooxindoles **8-10**.

A series of imidazole-based MDM2 inhibitors was designed by close examination of a model of the AP peptide bound to MDM2.[30] The imidazole scaffold was chosen to orientate the three substituents into the Phe19, Trp23, and Leu26 pockets, and to make favourable contacts with Val23. Initial examples, e.g. **11**, had modest inhibitory activity for MDM2. Addition of a hydrophilic group to the indole via a carboxamide link (**12**) gave a significant improvement in activity. Analysis of the X-ray co-crystal structure of MDM2 with **12** revealed that the carbonyl group makes water-bridged hydrogen bonds to the protein, whereas the morpholino group projects into solvent. Development of this series sought to take advantage of a possible interaction with His96, observed to stack

favourably with the chlorobenzyl group of **12**.[31] Introduction of an amide group at the 2-position of the imidazole, replacement of the 4-chlorobenzyl group with a 3-chlorophenyl substituent and simplification of the indole substituent to a 3-chlorophenyl group led to **13a**, which showed moderate MDM2-p53 inhibitory activity (Table 5). The corresponding acid **13b** showed improved activity. Modelling indicated that additional substitution on the aromatic rings would induce the ideal conformation for binding, as was demonstrated by the difluoro compound **13d** with excellent inhibitory activity. A further gain in potency was achieved by the replacement of the 5-phenyl substituent with a cyclohexyl group (**13e**),thus optimising interactions in the Phe19 pocket. The cellular activity was optimised by replacement of the carboxylic acid group with bioisosteric groups **13f-h**, the oxadiazoleamine **13h** showing the best cellular activity. The presence of a *tert*-butylacetamide group at R^1, as in **13i**, conferred the best combination of inhibitory activity and cellular activity. The latter property in this series is low compared with other series displaying low nanomolar potency in cell-free MDM2-p53 inhibition assays, possibly indicating poor cellular uptake.

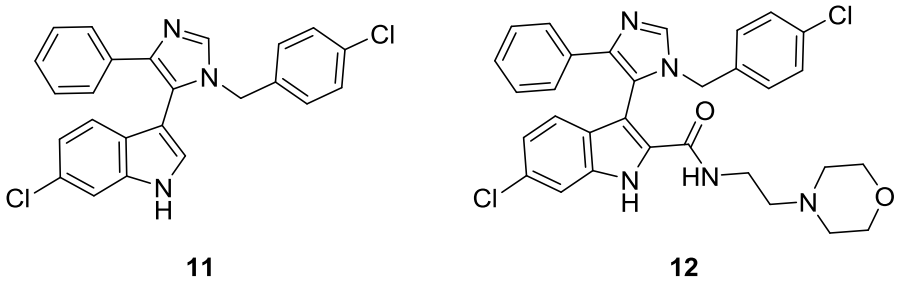

Figure 5: Chemical structures of imidazoles **11** and **12**.

Table 5: MDM2-p53 inhibitory activity and growth inhibitory activity of imidazoles **13**. [31]

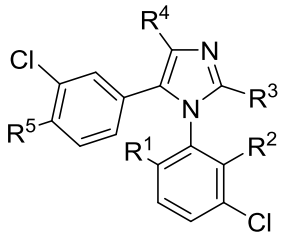

Compound	R^1	R^2	R^3	R^4	R^5	IC_{50}[a] (μM)	SJSA-1 IC_{50} (μM)
13a	H	H	Ph	-$CONHCH_3$	H	0.31	
13b	H	H	Ph	-CO_2H	H	0.12	N/A
13c	Me	H	3-MePh	-CO_2H	H	0.008	10.2
13d	H	F	Ph	-CO_2H	F	0.003	14.0
13e	H	F	*c*-hexane	-CO_2H	F	0.004	13.2
13f	H	F	*c*-hexane	-$CONH_2$	F	0.018	4.1
13g	H	F	*c*-hexane	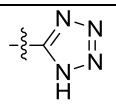	F	0.003	4.4
13h	H	F	*c*-hexane	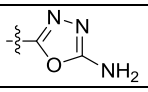	F	0.006	3.5
13i	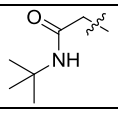	F	*c*-hexane	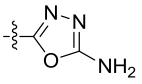	F	0.002	0.5

a) Time-resolved Förster resonance energy transfer (TR-FRET) assay

The substituted piperidines **14a** and **14b** were identified as hits with micromolar potency by a screening campaign at Merck using a MDM2-p53 fluorescence polarisation (FP) assay.[32] Optimisation of the piperazine amide moiety showed that replacement of the pyridine nitrogen with an alkoxy substituent gave improved potency, and the 2-methoxyethoxy substituent was taken into the next round of SAR (**14c**, Table 6). The DMPK profile of the series was addressed by the addition of substituents at the 2-position of the piperidine ring.[33] This modification had the additional advantage of favouring the bound conformation of the ring, resulting in additional potency: e.g., the 2-allyl derivative **14d** showed a 4-fold improvement in cell-free and cellular potency over **14c**. Additional polarity was introduced by dihydroxylation of **14a** as in **14f**. In this case, the more potent diastereoisomer showed improved potency and cellular activity against p53wt cell lines. Simplification of the substituent to 2-hydroxyethyl, as in **14g**, gave a modest improvement in potency and cellular activity.

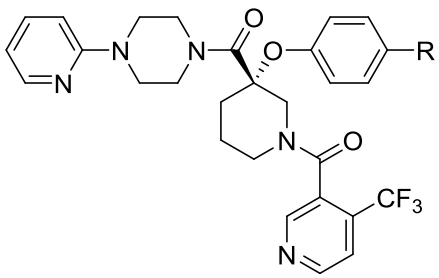

14a: R = CF_3, IC_{50} = 2.3 μM
14b: R = CH_3, IC_{50} = 1.5 μM

Figure 6: Chemical structures and MDM2 inhibitory activities of piperidines **14a** and **14b**.

Table 6: MDM2-p53 inhibitory activity and growth inhibitory activity of substituted piperazines **14**. [32]

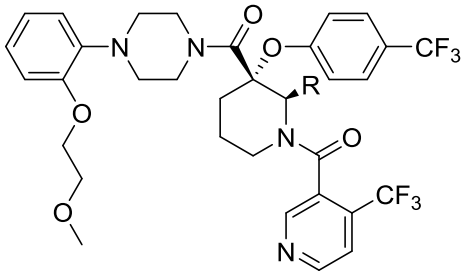

14

Compound	R	IC_{50} (nM)[a]	SJSA-1 IC_{50} (μM)
14c	H	169	4.7
14d	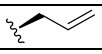	41	1
14e		24	1.2
14f	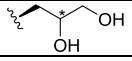	16	0.42
14g	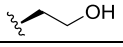	24	0.53

a) FP assay

Analysis of the X-ray structures of a number of MDM2 inhibitory chemotype by the Amgen group pointed to the importance of interactions with His96, which forms part of the Leu23 pocket, leading to improved potency, in addition to efficient occupation of the three hydrophobic pockets on MDM2 by the ligand. On this basis, the piperidone series of inhibitors was conceived, e.g. **15a** and **15b**.[34] Molecular modelling guided SAR studies, which sought to optimise the *N*-alkyl group, established the cyclopropylmethyl group as the most potent in the series.[35] The introduction of the (3*R*)-carboxyl group at C3 resulted in a 20-fold improvement in potency (**15b**), whereas the (3*S*)-diastereomer was 2-fold less potent. The importance of the interaction with His96 was confirmed by the loss of potency observed for the amide derivative **15d**, and the retention of potency for the isosteric tetrazole **15e**. Importantly, the authors noted a reduction in activity when the assays were

conducted in the presence of human serum, due to plasma protein binding. Guided by computational models, the introduction of an additional group to the R^1 substituent (e.g. *tert*-butyl ester **15f**) resulted in a 8-fold gain in potency, rationalised by the bulky group directing R^1 into the optimal conformation for binding. Similarly, the introduction of a methyl group at C3 (**15g**) resulted in a 2-fold improvement in potency by stabilising the bound conformation of the piperidone ring. The tetrazole analogue **15h** showed improved cell-free potency, but similar cellular potency. Enhanced cellular potency was achieved by replacing the R^1 substituent with 3-(2-hydroxypentyl) leading to **15i** (AM8553), a compound that showed promising *in vivo* PK and PD properties. *In vivo* efficacy was demonstrated, with tumour stasis observed on oral daily dosing at 150mg/kg, and oral twice daily 100 mg/kg, in an SJSA-1 mouse xenograft model.

Table 7: MDM2-p53 inhibitory activity and growth inhibitory activity of substituted piperidones **15a-i**. [34]

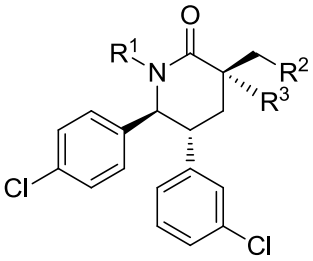

Compound	R^1	R^2	R^3	IC_{50} (nM)[a]	SJSA-1 EdU (10% HS[b]) IC_{50} (μM)
15a	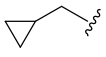		H	34.0 ± 5.8	3.35 ± 0.38
15b			H	6[c]	nd
15c	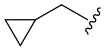	H	H	820 ± 280	nd
15d	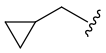		H	270 ± 70	nd
15e	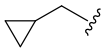		H	14 ± 4	nd
15f			H	4.2 ± 0.9	0.476 ± 0.087
15g	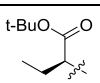			2.2 ± 0.7	0.19 ± 0.06
15h	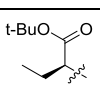	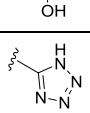		0.90 ± 0.21	0.17 ± 0.03
15i (AM8553)				1.1 ± 0.5	0.068 ± 0.016

a) HTRF assay; b) 10% human serum added to medium; c) K_D by surface plasmon resonance

Guided by an X-ray structure of **15i** bound to MDM2 (pdb: 4ERF, Figure 8), further optimisation of this chemotype focussed on the N-substituent with the aim of optimising interactions in the 'glycine shelf' region (Table 8).[36] Homologation of the alcohol group (**15j**) resulted in a modest improvement in cell free potency that did not transfer to the cellular potency. In contrast, the cyclopropylsulfonamide derivative **15k**, reversed sulfonamide **15l**, and sulfone **15m** (AMG 232) displayed improved cell-free potency and excellent growth inhibitory activity. The X-ray co-crystal structure of the sulfone **15n** (pdb: 4OCC, Figure 8) showed the ethyl R^1-group projecting into the Phe19 binding pocket, directed by the α-substituent. The sulfone group is situated close to the Gly58 CH suggesting a favourable interaction, accounting for the improved potency. Of the three modifications, the sulfone derivative showed the best stability in human hepatocytes and the lowest *in vivo* rat clearance, giving an acceptable half-life. *In vivo* efficacy was demonstrated with AMG 232 (**15m**) with complete tumour regression in SJSA-1 xenografts seen with oral daily dose 60 mg/kg, leading to this compound being selected for clinical trials.

Table 8: MDM2-p53 and growth inhibitory activity and PK properties of substituted piperidones **15i-n**. [36]

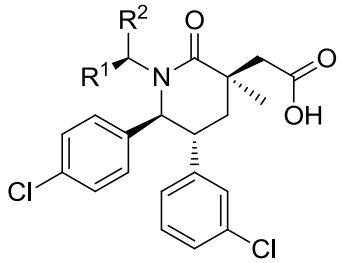

compound	R^1	R^2	IC_{50} (nM)[a]	SJSA-1 EdU (10% HS)[b] IC_{50} (nM)	hHep CL_{int} (μL/min/10^6 cells)[c]	Rat PK (iv, 0.5 mg/kg) CL (L/h/kg)/$t_{1/2}$(h)
15i	Et		1.1 ± 0.5	72 ± 14	3.0	1.2/3.5
15j	Et	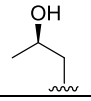	0.4 ± 0.08	150 ± 62	nd	nd
15k	*i*-Pr	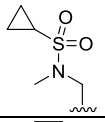	0.2 ± 0.06	6.5 ± 3.0	7.3	3.2/2.5
15l	*c*-Pr	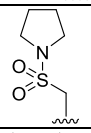	0.1 ± 0.02	4.4 ± 0.66	14	6.2/1.6
15m	*i*-Pr	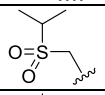	0.6 ± 0.4	9.1 ± 2.8	6.3	0.66/2.4
15n	Et	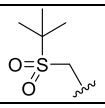	0.1 ± 0.04	3.0 ± 0.8	nd	nd

a) HTRF assay; b) 10% human serum added to medium; c) clearance in human hepatocytes.

Further modifications were pursued with the aim of replacing the carboxylic acid moiety, whilst retaining the favourable interaction with His96 (Table 9).[37] Replacement with carboxyl-substituted heterocycles, e.g. 2-pyridyl derivative **15p**, pyrazole **15q**, and thiazoles **15r** and **15s**, gave equipotent compounds. A hydrogen bond between the His96 NH and heterocycle N was observed in the co-crystal structures of **15p** and **15s**. The carboxylic acid group serves to modulate inhibition of cytochrome P450 monooxygenase (CYP) with the carboxymethyl derivative **15s** showing the best profile. Compound **15s** exhibited *in vivo* good mouse and rat PK, and activity in the SJSA-1 xenograft model, inducing tumour growth inhibition with oral daily dosing at 50 mg/kg.

Table 9: MDM2-p53 and growth inhibitory activity and PK properties of substituted piperidones **15.** [37]

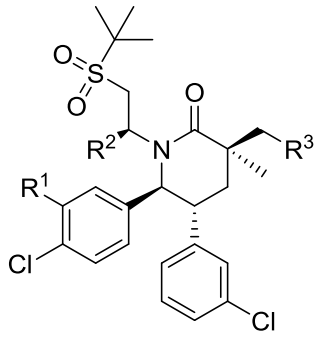

compound	R^1	R^2	R^3	IC_{50} (nM)[a]	SJSA-1 EdU (10% HS)[b] IC_{50} (nM)	hHep CL_{int} (µL/min/10^6 cells)[c]
15o	H	Et		0.10 ± 0.5	3 ± 1	N/A
15p	H	*c*-Pr	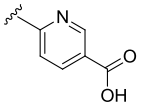	0.10 ± 0.01	5 ± 3	10
15q	H	*c*-Pr	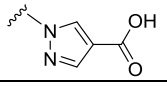	0.10 ± 0.01	4 ± 1	2.8
15r	F	*c*-Pr	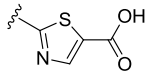	0.10 ± 0.01	4 ± 1	10.0
15s	F	*c*-Pr	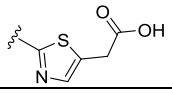	0.10 ± 0.01	16 ± 1	5.5

a) HTRF assay; b) 10% human serum added to medium; c) clearance in human hepatocytes.

In addition to the piperidinone series, a series of related morpholinones was identified with acceptable potency and cellular activity e.g. **16a** (Table 10).[38] Optimisation of this series was guided by the knowledge gained in the piperidone series.[39] Comparison of **16b** with the equivalent piperidone showed a 5-10 fold loss of potency, but better stability in hepatocytes derived from human and other mammalian species. Extensive SAR studies demonstrated the potency of *N*-arylsulfonamides, e.g. **16b**. However, time-dependent inhibition of CYP3A4 was observed for this sub-series. The sulfone series retained equivalent potency, e.g. **16c**, but without the CYP liability. Optimisation of the R^1 group revealed that the *N*-cyclopropylmethyl compound **16d** had the best combination of potency and low clearance in human hepatocytes. Mouse SJSA-1 xenograft experiments with **16d** showed tumour stasis with 100 mg/kg oral daily dosing.

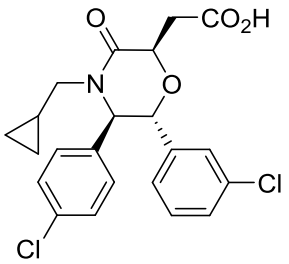

16a

Figure 7: Chemical structures of piperidinone **16a**.

Table 10: MDM2-p53 and growth inhibitory activity and PK properties of substituted morpholinones **16b-d**

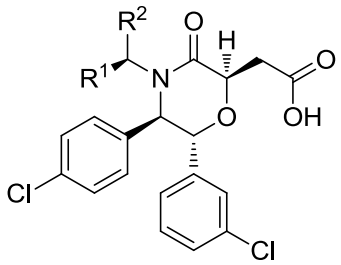

compound	R^1	R^2	HTRF IC_{50} (nM)[a]	SJSA-1 EdU (10% HS)[b] IC_{50} (nM)	hHep CL_{int} (μL/min/10^6 cells)	Rat PK (iv, 0.5 mg/kg) CL (L/h/kg)/$t_{1/2}$(h)
16a	*c*-Pr	H	290 ± 20	16700 ± 1900	nd	nd
16b	Et	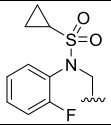	0.3 ± 0.1	35 ± 4	< 0.1	N/A
16c	Et	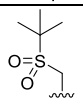	0.5 ± 0.3	37 ± 19	1.9	0.23/4.1
16d	*c*-Pr	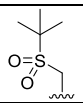	0.4 ± 0.1	25 ± 9	1.4	0.35/5.7

a) HTRF assay; b) 10% human serum added to medium.

Structural biology overview – common pharmacophore

Since the publication of the X-ray structure of Nutlin-2 bound to MDM2 [12], a number of structures have been added to the pdb, for a range of MDM2-p53 inhibitory chemotypes. These structures reveal a number of common features as shown in an overlay of the core structures of the Nutlin RG7112 **2g**, a spirooxindole scaffold **5h**, RG7388 **6a**, and piperidinone analogues of AMG 233 **15i** and **15n** (Figure 8A). The Trp23 pocket strongly favours a chloroaromatic group and each ligand has the

chlorine atom in a very similar position, occupying the lipophilic base of the pocket. The Leu26 is also occupied by a chloroaromatic group, with the chlorine atoms in each structure occuping a similar space and vector. The phenyl rings also occupy similar space regardless of the vector to the scaffold. The greatest structural diversity is seen in the Phe19 pocket that is filled by a saturated alkyl group, e.g. *tert*-butyl, in the structures shown. The His96 is seen to make favourable interactions with the carboxylic acid or carboxamide groups of the ligands, where present. Each scaffold bears a hydrophilic group, which occupies the glycine shelf for RG7388 analogue **6a** and piperidone **15i**, or overlay the Phe pocket for RG7112 **2g**, and project into solvent. The interactions for each ligand are summarised in Figure 9.

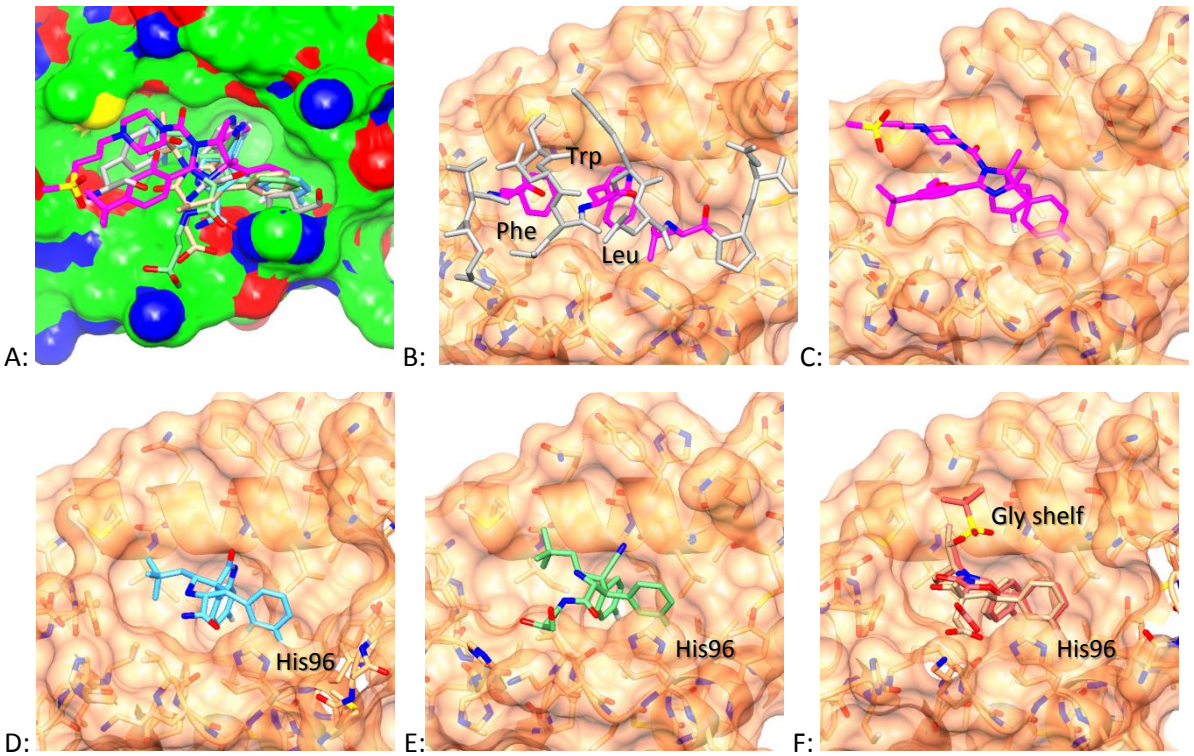

Figure 8: A: Overlay of MDM2-ligand complex X-ray crystal structures; B: 1YCR – p53 peptide (grey and magenta); C: 4IPF – RG7112 **2g** (magenta), D: 3LBL – spirooxindole scaffold **5h** (light blue); E: 4JRG – RG7388 analogue **6a** (green); F: 4ERF and 4OCC – AMG-232 analogues **15i** (pale brown) and **15n** (pale crimson).

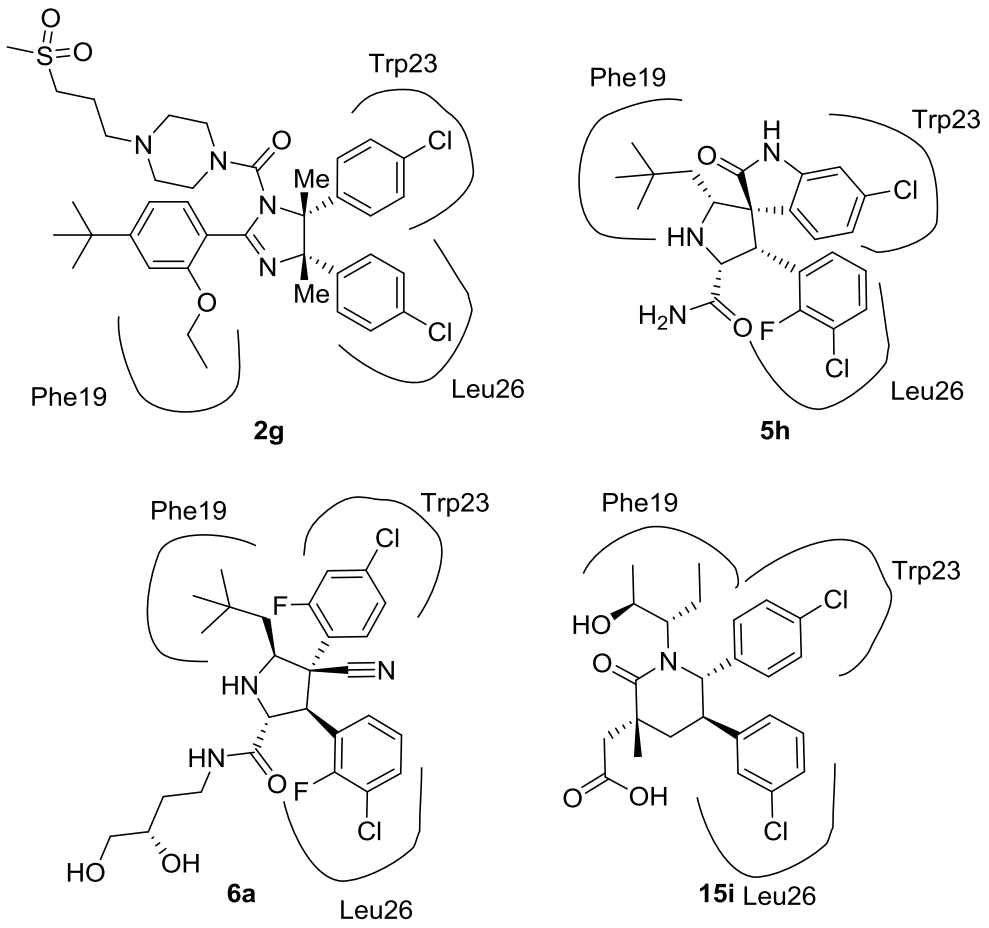

Figure 9: Schematic showing the occupancy of the MDM2 Phe19, Trp23, and Leu26 binding pockets by ligands **2g**, **5h**, **6a**, and **15i**.

Clinical Trials

The first full publication of a phase 1 clinical trial of an MDM2-p53 inhibitor detailed the activity of RG7112 **2g** in liposarcoma patients.[17] Patients received RG7112 **2g** (1440 mg/m² per day, oral dosing) for 10 days in up to three 28-day cycles. Within the group, 18 from 20 patients had *TP53* wild-type tumours and two carried missense *TP53* mutations. Among the patients assessed, 14 from 17 had *MDM2* gene amplification. An initial response to therapy was observed in 16 from 20 patients as partial response or stable disease. Interpatient variability in pharmacokinetics allowed a linear relationship to be established between drug exposure and the PD markers TUNEL (for apoptosis) and MIC-1 (for p53 activation). Some toxicity was observed including neutropenia and thrombocytopenia, thought to be related to p53 activation. The poor PK profile of the Nutlin analogue RG7112 **2g** can be predicted from the compound's high molecular weight (MW) and lipophilicity. The follow-up compound RG7388 **6g** currently in trials has lower MW and lipophilicity and has replaced **2g** in clinical studies.

Future Perspective

To date at least seven chemically diverse MDM2-p53 inhibitors are in Phase I or Phase II clinical trials for the treatment of solid and haematological malignancies. Also, a number of combination studies with chemotherapy and targeted agents are running concurrently. Twenty years have elapsed between the initial characterisation of MDM2 in 1992[4] and the first clinical data from a small molecule inhibitor. The data are encouraging and suggest that MDM2-p53 inhibition can be a useful therapy for p53 wild-type tumours. The data also reinforce the challenges of designing an inhibitor of a lipophilic protein-protein interaction, whilst retaining favourable pharmaceutical properties. Given the range of chemotypes reported, it is likely that one or more MDM2-p53 inhibitor will be successful in the near future.

Executive Summary

- Overexpression of MDM2 functionally inactivates p53 in p53 wild-type tumours.
- Inhibition of MDM2-p53 protein-protein interaction results in activation of p53 in cells
- The MDM2-p53 protein-protein interaction is a well validated and attractive target for small-molecule therapeutics
- A number of series of MDM2-p53 inhibitors have been discovered, based on different chemotypes. Potency and in vivo efficacy have been demonstrated for compounds with acceptable pharmaceutical properties.
- MDM2-p53 inhibitors have entered clinical trials in solid and haematological malignancies as single agents and in combination with targeted agents
- RG7112 showed promising activity in a Phase 1 trial, but interpatent variablity in pharmacokinetics was observed

Key Terms

p53 - the tumour suppressor protein p53, a transcription factor

MDM2 - Mouse Double Minute 2, an E3 ligase, transcriptional target for p53

Protein-protein interaction - the surface to surface interaction of two proteins that may include sites able to bind small molecules

SJSA-1 - osteosarcoma tumour cell-line that is MDM2 amplified and p53 wild type, used for *in vitro* cell assays and xenograft models

Acknowledgements

The authors thank Cancer Research UK and Newcastle University for financial support.

Disclosure

BZ, BTG, and IRH are part of a collaborative research project between Newcastle University and Astex Pharmaceuticals Ltd towards small-molecule MDM2-p53 inhibitors.

References

1. Lane DP. Cancer. p53, guardian of the genome. Nature, 358, 15-16 (1992).
2. Bode AM, Dong Z. Post-translational modification of p53 in tumorigenesis. Nat Rev Cancer, 4(10), 793-805 (2004).
3. Vousden KH, Lu X. Live or let die: the cell's response to p53. Nat. Rev. Cancer, 2, 594-604 (2002).
4. Oliner JD, Kinzler KW, Meltzer PS, George DL, Vogelstein B. Amplification of a Gene Encoding a P53-Associated Protein in Human Sarcomas. Nature, 358(6381), 80-83 (1992).
5. Oliner JD, Pietenpol JA, Thiagalingam S, Gvuris J, Kinzler KW, Vogelstein B. Oncoprotein Mdm2 Conceals the Activation Domain of Tumor Suppressor-P53. Nature, 362(6423), 857-860 (1993).
6. Momand J, Zambetti GP, Olson DC, George D, Levine A. The mdm-2 oncogene product forms a complex with p53 protein and inhibits p53-mediated transactivation. Cell, 69, 1237-1245 (1992).
7. Momand J, Wu H-H, Dasgupta G. MDM2 -- master regulator of the p53 tumor suppressor protein. Gene, 242(1-2), 15-29 (2000).
8. Toledo F, Wahl GM. Regulating the p53 pathway: in vitro hypotheses, in vivo veritas. Nat Rev Cancer, 6(12), 909-923 (2006).
9. Picksley SM, Vojtesek B, Sparks A, Lane DP. Immunochemical analysis of the interaction of p53 with MDM2; - fine mapping of the MDM2 binding site on p53 using synthetic peptides. Oncogene, 9, 2523-2529 (1994).
10. Böttger V, Böttger A, Howard SF et al. Identification of novel mdm2 binding peptides by phage display. Oncogene, 13(10), 2141-2147 (1996).
11. Garcia-Echeverria C, Chene P, Blommers MJJ, Furet P. Discovery of potent antagonists of the interaction between human double minute 2 and tumor suppressor p53. J. Med. Chem., 43(17), 3205-3208 (2000).
12. Kussie PH, Gorina S, Marechal V et al. Structure of the MDM2 oncoprotein bound to the p53 tumor suppressor transactivation domain. Science, 274, 948-953 (1996).
13. Weber L. Patented inhibitors of p53–Mdm2 interaction (2006 – 2008). Exp. Opin. Ther. Patents, 20(2), 179-191 (2010).
14. Khoury K, Popowicz GM, Holak TA, Domling A. The p53-MDM2/MDMX axis - A chemotype perspective. MedChemComm, 2(4), 246-260 (2011).
15. Zak K, Pecak A, Rys B et al. Mdm2 and MdmX inhibitors for the treatment of cancer: a patent review (2011 – present). Expert Opin. Ther. Patents, 23(4), 425-448 (2013).
16. Watson AF, Liu J, Bennaceur K et al. MDM2-p53 protein-protein interaction inhibitors: A-ring substituted isoindolinones. Bioorg. Med. Chem. Lett., 21(19), 5916-5919 (2011).
17. Ray-Coquard I, Blay J-Y, Italiano A et al. Effect of the MDM2 antagonist RG7112 on the P53 pathway in patients with MDM2-amplified, well-differentiated or dedifferentiated

liposarcoma: an exploratory proof-of-mechanism study. The Lancet Oncology, 13(11), 1133-1140 (2012).
18. Vassilev LT, Vu BT, Graves B et al. In Vivo Activation of the p53 Pathway by Small-Molecule Antagonists of MDM2. Science, 303, 844-848 (2004).
19. Vu B, Wovkulich P, Pizzolato G et al. Discovery of RG7112: A Small-Molecule MDM2 Inhibitor in Clinical Development. ACS Med. Chem. Lett., 4(5), 466-469 (2013).
20. Zaytsev A, Dodd B, Magnani M et al. Searching for Dual Inhibitors of the MDM2-p53 and MDMX-p53 Protein–Protein Interaction by a Scaffold-Hopping Approach. Chemical Biology & Drug Design, n/a-n/a (2014).
21. Miyazaki M, Kawato H, Naito H et al. Discovery of novel dihydroimidazothiazole derivatives as p53–MDM2 protein–protein interaction inhibitors: Synthesis, biological evaluation and structure–activity relationships. Bioorg. Med. Chem. Lett., 22(20), 6338-6342 (2012).
22. Miyazaki M, Naito H, Sugimoto Y et al. Lead optimization of novel p53-MDM2 interaction inhibitors possessing dihydroimidazothiazole scaffold. Bioorg. Med. Chem. Lett., 23(3), 728-732 (2013).
23. Yu S, Qin D, Shangary S et al. Potent and Orally Active Small-Molecule Inhibitors of the MDM2-p53 Interaction. J. Med. Chem., 52(24), 7970-7973 (2009).
24. Shangary S, Qin D, McEachern D et al. A novel orally active MDM2 inhibitor (MI-219) activates the p53 pathway and is selectively toxic to tumor cells. Mol. Cancer Ther., 6(12), 3518S-3518S (2007).
25. Zhao Y, Liu L, Sun W et al. Diastereomeric Spirooxindoles as Highly Potent and Efficacious MDM2 Inhibitors. J. Am. Chem. Soc., 135(19), 7223-7234 (2013).
26. Zhao Y, Yu S, Sun W et al. A Potent Small-Molecule Inhibitor of the MDM2–p53 Interaction (MI-888) Achieved Complete and Durable Tumor Regression in Mice. J. Med. Chem., 56(13), 5553-5561 (2013).
27. Ding Q, Zhang Z, Liu J-J et al. Discovery of RG7388, a Potent and Selective p53–MDM2 Inhibitor in Clinical Development. J. Med. Chem., 56(14), 5979-5983 (2013).
28. Zhang Z, Ding Q, Liu J-J et al. Discovery of potent and selective spiroindolinone MDM2 inhibitor, RO8994, for cancer therapy. Bioorg. Med. Chem., 22(15), 4001-4009 (2014).
29. Zhang Z, Chu X-J, Liu J-J et al. Discovery of Potent and Orally Active p53-MDM2 Inhibitors RO5353 and RO2468 for Potential Clinical Development. ACS Med. Chem. Lett., 5(2), 124-127 (2013).
30. Furet P, Chène P, De Pover A et al. The central valine concept provides an entry in a new class of non peptide inhibitors of the p53–MDM2 interaction. Bioorg. Med. Chem. Lett., 22(10), 3498-3502 (2012).
31. Vaupel A, Bold G, De Pover A et al. Tetra-substituted imidazoles as a new class of inhibitors of the p53–MDM2 interaction. Bioorg. Med. Chem. Lett., 24(9), 2110-2114 (2014).
32. Ma Y, Lahue BR, Shipps Jr GW, Brookes J, Wang Y. Substituted piperidines as HDM2 inhibitors. Bioorg. Med. Chem. Lett., 24(4), 1026-1030 (2014).
33. Ma Y, Lahue BR, Gibeau CR et al. Pivotal Role of an Aliphatic Side Chain in the Development of an HDM2 Inhibitor. ACS Med. Chem. Lett., 5(5), 572-575 (2014).
34. Michelsen K, Jordan JB, Lewis J et al. Ordering of the N-Terminus of Human MDM2 by Small Molecule Inhibitors. J. Am. Chem. Soc., 134(41), 17059-17067 (2012).
35. Rew Y, Sun D, Gonzalez-Lopez De Turiso F et al. Structure-Based Design of Novel Inhibitors of the MDM2–p53 Interaction. J. Med. Chem., 55(11), 4936-4954 (2012).
36. Sun D, Li Z, Rew Y et al. Discovery of AMG 232, a Potent, Selective, and Orally Bioavailable MDM2–p53 Inhibitor in Clinical Development. J. Med. Chem., 57(4), 1454-1472 (2014).
37. Gonzalez AZ, Li Z, Beck HP et al. Novel Inhibitors of the MDM2-p53 Interaction Featuring Hydrogen Bond Acceptors as Carboxylic Acid Isosteres. J. Med. Chem., 57(7), 2963-2988 (2014).

38. Gonzalez-Lopez de Turiso F, Sun D, Rew Y et al. Rational Design and Binding Mode Duality of MDM2–p53 Inhibitors. J. Med. Chem., 56(10), 4053-4070 (2013).
39. Gonzalez AZ, Eksterowicz J, Bartberger MD et al. Selective and Potent Morpholinone Inhibitors of the MDM2–p53 Protein–Protein Interaction. J. Med. Chem., 57(6), 2472-2488 (2014).